Fabrication of WO_3 Nanoflakes by a Dealloying-based Approach

Zhifu Liu,* Toshinari Yamazaki, Yanbai Shen, Dan Meng, Toshio Kikuta, and Noriyuki Nakatani
School of Engineering, University of Toyama, 3190 Gofuku, Toyama 930-8555

(Received December 10, 2007; CL-071370)

We demonstrate the fabrication of WO_3 nanoflakes by dealloying with subsequent thermal oxidation. Sputtered amorphous $W_{0.68}Cu_{0.32}$ alloy films were dealloyed in HNO_3 solution where Cu was selectively removed and W self-assembled into cross-linked cubic phase W nanoflakes. This kind of W nanoflakes was transformed to monoclinic WO_3 nanoflakes by thermal oxidation at 500 °C. Gas sensor made using the WO_3 nanoflakes showed promising NO_2-sensing performance.

High surface area nanostructural materials are of great interest because of their ability to fulfill the demand of high efficiency and/or activity in a wide range of applications such as catalysis,[1] chemical and biosensors,[2] solar cells,[3] and so forth. Great efforts have been taken to explore new synthesis methods and to control the formation of nanostructures to satisfy certain application. In recent years, dealloying process has been applied to synthesize high surface area nanoporous metal materials including noble metals, such as Pt,[4] Au,[5] and transition metals, such as Ni[6] and Cu.[7] During the dealloying process, phase separation at the solid–electrolyte interface and dissolution of the more active component occur simultaneously. The remaining species self-assemble through surface diffusion, forming nanoporous metals.[4–8] Metals are natural source materials for inorganic materials such as oxides, nitrides, and sulfides. In this context, it is possible to transform the nanostructural metals, especially transition-metal materials, obtained by dealloying to oxides, nitrides, or sulfides, which succeed the framework of the metals, through controlled heat treatment in specific atmosphere.

Tungsten oxide (WO_3) is a versatile semiconductor material with interesting optical and electrical properties which finds applications in photoelectrochromic devices, chemical sensors, photocatalysis, and so forth.[9–11] For these applications, great interest arises in synthesis of high surface area WO_3 to obtain enhanced performance.[12–14] Herein, we report on the fabricate of high surface area WO_3 films composed of nanoflakes through dealloying W–Cu films in diluted acid solution followed by a controlled thermal oxidation process.

The source $W_{0.68}Cu_{0.32}$ films were deposited using a DC sputtering method. Pure W disk attached with Cu chips was used as sputtering target. The $W_{0.68}Cu_{0.32}$ films with thickness of about 1 μm were deposited on SiO_2/Si substrate at room temperature in Ar at a discharge pressure of 10 mTorr. The sputtered alloy film (10 × 5 mm in area) was immersed in 20 mL of 0.5 M aqueous HNO_3 solution and dealloyed for 24 h at room temperature. Then, the films were rinsed using deionized water and blow-dried in warm air. To obtain WO_3, the dealloyed films were oxidized at 500 °C for 8 h in air at a heating/cooling rate of 2 °C/min. The products were characterized using X-ray diffraction (XRD, Shimadzu XRD-6100), field emission scanning electron microscopy (FESEM, JSM-6700F) equipped with energy dispersive X-ray spectroscopy (EDS), and transmission electron microscopy (TEM, TOPCON EM-002B).

The XRD patterns of the as-deposited and dealloyed films are shown in Figure 1a. The as-deposited $W_{0.68}Cu_{0.32}$ films are amorphous. After dealloyed in HNO_3 solution, the film crystallized. The dealloyed film shows diffraction peaks at about 35.5 and 40°, respectively. These peaks can be assigned to the diffraction of the cubic-phase tungsten (JCPDS Card No. 47-1319). Figure 1b is a FESEM image of the dealloyed film. Cross-linked nanoflakes are obtained after dealloying the alloy film in HNO_3 solution. These nanoflakes have flat surface and are less than 100 nm in thickness.

Normally, the chemical potential difference is the driving force of the dissolution of the more active species during dealloying process. The standard equilibrium potentials for the W^{6+}/W and Cu^{2+}/Cu couples are −0.09 V (SHE) and 0.34 V (SHE), respectively. So, Cu is thermodynamically more stable than W by 0.43 V. However, Cu is selectively dissolved in HNO_3 solution. Other researchers also observed this kind of phenomenon, which was ascribed to the formation of a passive oxide layer on the surface of active metal.[6] In the present W–Cu alloy system, it is possible that a protection layer is formed on W in HNO_3 solution. As a result, W is passivated and is kinetically stable.[15] The dealloying induced surface strain and active surface diffusion result in the formation of these nanoflakes.[16]

The W nanoflakes can be precursor for preparing tungsten-based oxides, sulfides, and nitrides nanostructures. We transformed the W nanoflakes to WO_3 nanoflakes by annealing at 500 °C in air with a well-controlled temperature process. Figure 2 shows the FESEM image of the oxidized product. Inset in Figure 2 is the corresponding XRD pattern. It is shown that the products succeed the skeleton of the metal nanoflakes and the flake structure is kept. But the edge of the nanoflakes is no longer sharp after thermal oxidation because of thermal diffusion. The

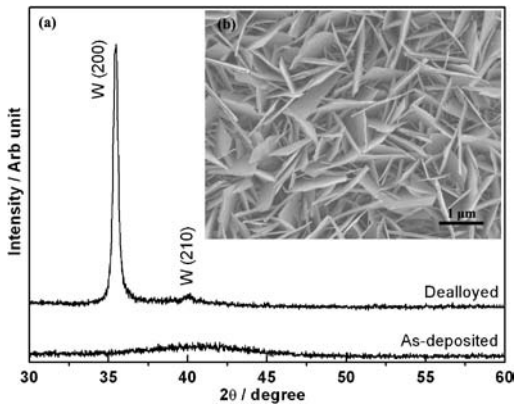

Figure 1. (a) XRD patterns of as-deposited and dealloyed films; (b) FESEM image of the film after dealloyed in HNO_3 solution for 24 h.

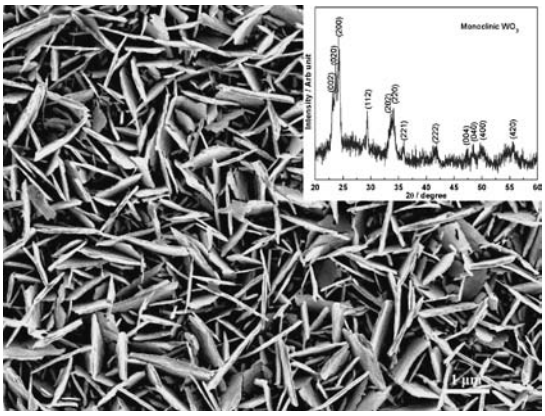

Figure 2. FESEM image of WO_3 nanoflakes obtained by annealing the delloyed film at 500 °C in air. Inset is the corresponding XRD pattern.

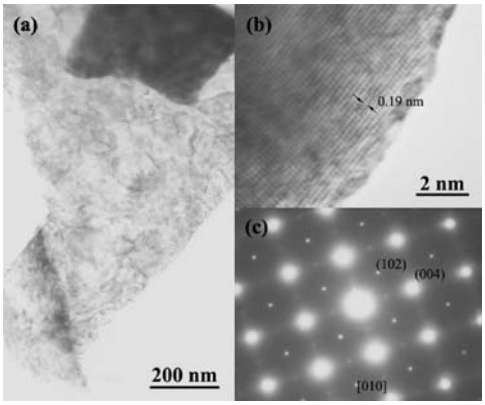

Figure 3. (a) TEM image, (b) HRTEM image, and (c) SAED pattern of the WO_3 nanoflake.

XRD pattern indicates that a kind of monoclinic phase WO_3 nanoflakes have been obtained (JCPDS Card No. 43-1035). Figure 3a shows a TEM image of the WO_3 nanoflake. A HRTEM image and a SAED pattern are shown in Figures 3b and 3c, respectively. The lattice fringe can be clearly seen from the HRTEM image, implying the good crystallization of the nanoflakes. Calculation shows a lattice spacing of 0.19 nm, which corresponds to the (004) lattice plane of the monoclinic WO_3. The SAED of the nanoflakes represents a uniform pattern of the monoclinic crystal phase with a [010] diffraction zone axis.

This kind of high surface area WO_3 nanoflakes is very good candidate for gas sensor, photochemical device, and catalysis applications. The NO_2-sensing of the WO_3 nanoflakes was investigated in the present work. Figure 4 shows the dynamic responses of the WO_3 nanoflake-based sensor to NO_2 gas at 200 °C. A diagram of the WO_3 nanoflake-based gas sensor device is also shown inset in Figure 4. Pt was deposited on top of the nanoflakes as electrodes. The nanoflake film with an area of 4×2 mm was exposed to the NO_2 gas. The sensor show reversible responses to the NO_2 pulses. The response increases with the increase of NO_2 concentration. The sensor responds fast, for example, the response time (time for reaching 90% of the total sensitivity) is 56 s to 20 ppm NO_2 gas at 200 °C, which

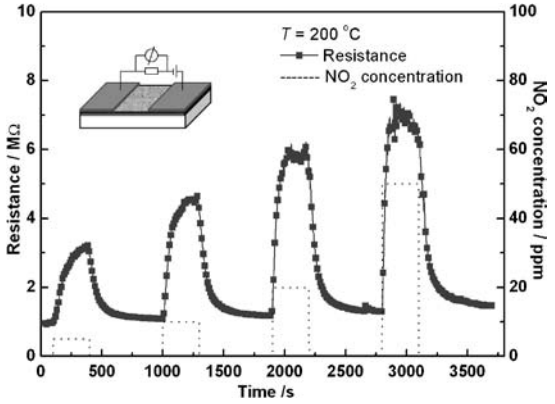

Figure 4. Dynamic responses of the WO_3 nanoflakes to NO_2 pulses at 200 °C. A diagram of the WO_3 nanoflake-based sensor device is also shown inset in Figure 4.

is less than tenth of that of conventional sputtered WO_3 thin film sensor.[17] The cross-linked feature of the thin nanoflakes shortens the electron diffusion distance into bulk, leading to the quick response of the gas sensor. Furthermore, the high surface area of WO_3 nanoflakes largely increases the surface active sites, which is also an advantage for gas sensor application.

In summary, this work introduced a method for synthesis high surface area WO_3. Dealloying the sputtered amorphous W–Cu alloy film in HNO_3 solution resulted in the formation of W nanoflakes. WO_3 nanoflakes were obtained by oxidizing the W nanoflakes in a controlled heat-treatment process. Gas sensor made using the WO_3 nanoflakes showed promising NO_2-sensing performance.

References and Notes

1 J. Zhang, K. Sasaki, E. Sutter, R. R. Adzic, *Science* **2007**, *315*, 220.
2 C. S. Rout, A. Govindaraj, C. N. R. Rao, *J. Mater. Chem.* **2006**, *16*, 3936; F. Patolsky, G. F. Zheng, C. M. Lieber, *Anal. Chem.* **2006**, *78*, 4260.
3 E. Lancelle-Beltran, P. Prene, C. Boscher, P. Belleville, P. Buvat, C. Sanchez, *Adv. Mater.* **2006**, *18*, 2579.
4 J. C. Thorp, K. Sieradzki, L. Tang, P. A. Crozier, A. Misra, M. Nastasi, D. Mitlin, S. T. Picraux, *Appl. Phys. Lett.* **2006**, *88*, 033110.
5 Y. Ding, Y. Kim, J. Erlebacher, *Adv. Mater.* **2004**, *16*, 1897.
6 L. Sun, C.-L. Chien, P. C. Searson, *Chem. Mater.* **2004**, *16*, 3125.
7 H.-B. Lu, Y. Li, F.-H. Wang, *Scripta Mater.* **2007**, *56*, 165.
8 J. Erlebacher, M. J. Aziz, A. Karma, N. Dimitrov, K. Sieradzki, *Nature* **2001**, *410*, 450.
9 S. Berger, H. Tsuchiya, A. Ghicov, P. Schmuki, *Appl. Phys. Lett.* **2006**, *88*, 203119.
10 M. Akiyama, J. Tamaki, N. Miura, N. Yamazoe, *Chem. Lett.* **1991**, 1611.
11 Y. Guo, X. Quan, N. Lu, H. Zhao, S. Chen, *Environ. Sci. Technol.* **2007**, *41*, 4422.
12 J. Zhou, Y. Ding, S. Z. Deng, L. Gong, N. S. Xu, Z. L. Wang, *Adv. Mater.* **2005**, *17*, 2107.
13 G. Wang, Y. Ji, X. Huang, X. Yang, P. I. Gouma, M. Dudley, *J. Phys. Chem. B* **2006**, *110*, 23777.
14 B. Zhang, C. Cao, H. Qiu, Y. Xu, Y. Wang, H. Zhu, *Chem. Lett.* **2005**, *34*, 154.
15 E. Lassner, W. D. Schubert, *Tungsten: Properties, Chemistry, Technology of the Element, Alloys and Chemical Compounds*, Kluwer Academic, New York, **1998**, p. 124.
16 Z. Liu, T. Yamazaki, Y. Shen, D. Meng, T. Kikuta, N. Nakatani, T. Kawabata, *J. Phys. Chem. C*, **2008**, *112*, 1391.
17 Z. Liu, T. Yamazaki, Y. Shen, T. Kikuta, N. Nakatani, *Sens. Actuators B* **2007**, *128*, 173.

Published on the web (Advance View) February 9, 2008; doi:10.1246/cl.2008.296